

# Experimental Measurement of Single-Phase Liquid Heat Transfer in a Curved Microtube Using Thermochromic Liquid Crystal

**Qian You, Yanfeng Fan**

<sup>1</sup>Concordia University, Department of Mechanical and Industrial Engineering  
1455 de Maisonneuve Blvd. W, Montreal, Quebec, Canada, H3G 1M8  
q\_you@encs.concordia.ca

**Ibrahim Hassan**

Texas A&M University at Qatar, Department of Mechanical Engineering  
P.O. Box 23874, Doha, Qatar  
ibrahim.hassan@qatar.tamu.edu

**Abstract-** The present work is to experimentally investigate the single-phase liquid heat transfer using un-encapsulated Thermochromic Liquid Crystal (TLC) technique. To the best of the authors' knowledge, this work is the first trial of using the TLC with a micro-curved tube. The objective of experiment was not met, however in this paper; we are reporting the experimental challenges to be considered in future studies. The experiments are conducted on two sizes of 90° bended microtubes with hydraulic diameters ( $D_h$ ) of 1.194 mm and 0.838 mm, respectively. The radius ratios, defined as the ratio of curvature radius of the test tube and its hydraulic radius ( $2R_c/D_h$ ), are 6.8 and 9.1 respectively. The dielectric fluid FC-72 is selected as the working flow. The inlet temperature maintains around 37°C and Re number varies from 4000 to 5500. The uniform heat flux ( $q''$ ) is applied to the microtube surface varying from 5 to 7 kW/m<sup>2</sup>. Un-encapsulated TLC is coated on the curved microtube surface for surface temperature measurement, and the tube surface temperature map is then illustrated. The stream-wise local Nu numbers against the Re number and heat fluxes for both microtubes are presented. It is found that the heat transfer coefficient in the curved portion of microtube enhanced by Dean Vortices. The maximum local Nusselt number appears at the turning angle between 40° and 60°.

**Keywords:** curved microtube, TLC, single-phase liquid, Heat Transfer

## Nomenclature

$C_p$  specific heat, J/(kg·K)  
 $D_h$  hydraulic diameter, mm  
 $D_{out}$  outer diameter of microtube, mm  
 $E$  enhancement factor  
 $I$  current, A  
 $K$  thermal conductivity, W/(m·K)  
 $L$  microtube length, mm  
 $L_h$  heated length, mm  
 $O$  ovalization  
 $Q$  volumetric flow rate, ml/min  
 $q''$  heat flux, kW/m<sup>2</sup>  
 $R_c$  radius of curvature, mm  
 $T$  temperature, °C  
 $V$  voltage, V  
 $x$  axial location, mm

$x_o$  location of the clip near the inlet, mm  
 $x_1$  axial location of ROI near the inlet, mm

## Dimensionless Number

$De$  Dean number,  $De = Re \times (D_h/2R_c)^{0.5}$   
 $Nu$  Nusselt number  
 $Re$  Reynolds number

## Subscript

$f$  fluid  
 $in$  inlet  
 $out$  outlet  
 $w$  wall  
 $x$  local value

## Abbreviation

CCD	charge-coupled device
ROI	Region of Interest
TLC	Thermochromic Liquid Crystal

## Greek

$\theta$	turning angle, °
----------	------------------

## 1. Introduction

Curved channels have been widely studied on heat transfer behaviour since last century. Dean (1927 and 1928) as one of pioneers did the analytical investigation on the secondary flow in a curved pipe. He described the vortices (named as Dean Vortices after his investigation) and introduced Dean Number ( $De$ ) in order to measure the strength of the secondary flow. Later, many researchers (Dravid et al., 1971; Mori and Nakayama, 1965; Mori et al., 1971) interested in the heat transfer studies in curved channels or coiled tubes. They all confirmed the secondary flow increased the flow resistance and the heat transfer in curved configuration. In recent years, as MEMS technology develops rapidly, curved microchannels attract more attentions on flow behaviours and heat transfer investigation (Yang et al., 2005; Al-Halhouli and Biittgenbach, 2010; Chu et al., 2012). For example, in micro heat exchangers, the curved microchannels have been considered as important parts for connecting, changing the flow direction or extending the flow path length. On the other hand, the heat transfer in curved microchannels is different from one in straight configuration due to the secondary flow (Mudawar, 2011). Sturgis and Mudawar (1991) experimentally investigated the heat transfer enhancement of single-phase fully-developed turbulent flow in a small curved rectangular channel. They concluded that Dean Vortices and the maximum velocity shift toward the outer wall were the main mechanisms for the heat transfer enhancement in small curved channels. Xi et al. (2010) carried on experiments to study the single-phase flow characteristics and the heat transfer phenomena in swirl microtubes with various hydraulic diameters at  $Re \leq 1800$ . They compared the experimental results with Dravid's correlations (Dravid et al., 1971). However, they indicated that the correlation proposed in conventional size couldn't predict the heat transfer in micro-size swirl tubes.

By concluding previous works on curved microchannels, most of researches were performed in large radius ratio ( $2R_c/D_h > 300$ ) curved microchannels on heat transfer investigation. However, in a compact area, small radius ratio ( $2R_c/D_h < 10$ ) is more desired. The corresponding studies are quite limited. Unlike straight microchannel researches, the traditional thermocouple measurement is not suitable for small radius ratio curved configuration anymore due to the limited space. The un-encapsulated Thermochromic Liquid Crystal (TLC) technique which has been studied comprehensively by Muwanga and Hassan (2006) is adopted to measure the curved surface temperature. Hence, this paper aims to the fundamental investigation on single-phase liquid heat transfer in curved microtubes with small curvature radii by using TLC measurement methodology.

## 2. Experiment Methodology and Data Reduction

### 2. 1. Experimental Facility and Test Section

Fig. 1(a) shows the test facility, which includes a closed working flow loop for experiments, a water flow loop for maintaining the inlet temperature, a degassing loop and a set of data acquisition system. The dielectric liquid FC-72 is selected as working fluid, and degassed before each measurement. The current facility is similar to the setup of Muwanga and Hassan (2006) and calibrated by them. Fig. 1(b) illustrates the test section. Two sizes of  $90^\circ$  bended stainless steel microtubes with equal length of straight portions at both ends are used for single-phase liquid heat transfer study. Their geometrical parameters are listed in Table. 1. Two clips are placed at both ends to provide uniform heat flux on the tube surface. The location of the clip near the inlet is set as  $x_0 = 0$  mm. There is an area highlighted by dish lines in Fig. 1(b) named as Region of Interest (ROI). In this area, the curved portion of microtube is monitored by a Sony CCD camera, and TLC is applied on this area for surface temperature measurement. The axial location of ROI near the inlet is set as  $x_1$ . Two T-type thermocouples are located outside of ROI for heat loss estimation.

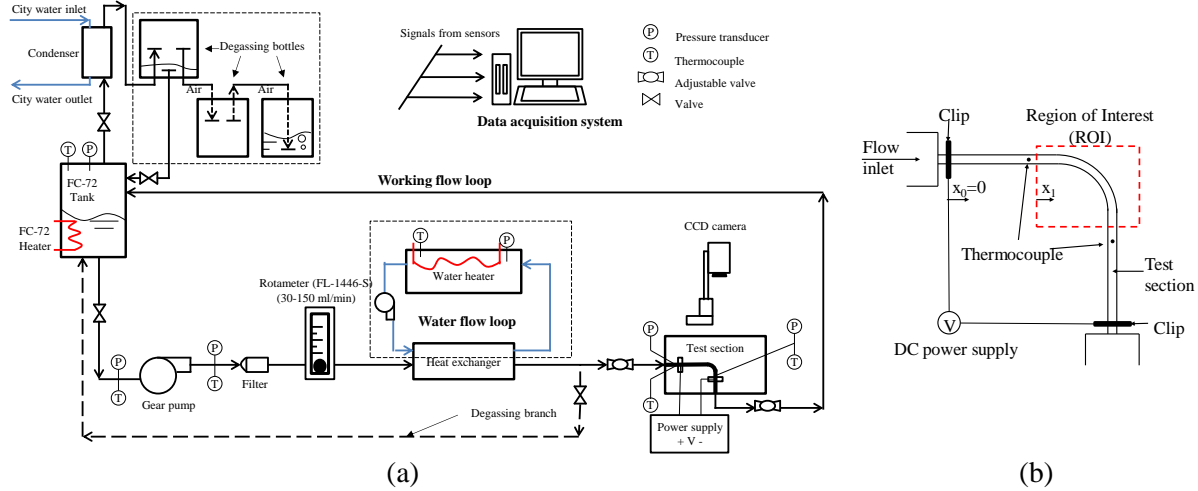


Fig. 1. (a) Experimental facility (b) Test section (not to scale)

## 2. 2. TLC Methodology and Test Matrix

In current study, un-encapsulated TLC is sprayed uniformly on the top surface of curved microtubes by airbrush. To qualify the TLC spray, the calibration is a must-have step. During the calibration stage, the CCD camera captures RGB images ( $640 \times 480$  pixels) with respect to the inlet temperature increment. Then, the color images are converted to HUE images ( $640 \times 480$  pixels) in LabView. The temperature respond range of TLC in current study is from  $35 \text{ }^\circ\text{C}$  to  $49 \text{ }^\circ\text{C}$ , and its color varies as temperature increases. The calibration is performed in this range. A user-defined MATLAB is used to create calibration curves for each interested area. The coating and the calibration methodologies refer to the comprehensive study on TLC measurement done by Muwaga and Hassan (2006). If most calibration curves are qualified, the TLC can be used for measurement. An example of calibration curve is shown in Fig. 2. During the experiment stage, the inlet temperature is maintained around  $37 \text{ }^\circ\text{C}$ , and desired heat fluxes are applied for testing. The test matrices in both curved microtubes are identical, Re number varies from 4000 to 5500. During the experiments, the inlet temperature maintains around  $37 \text{ }^\circ\text{C}$ . The heated length ( $L_h$ ) is 72 mm, and uniform  $q''$  are applied on the tube surface from 5 to  $7 \text{ kW/m}^2$ . During the calibration and the measurement, the CCD camera should be kept at the same position.

Table. 1. Geometrical parameters of curved microtubes

Tube No.	#1	#2
Hydraulic diameter, $D_h$ (mm)	1.194	0.838
Outer diameter, $D_{out}$ (mm)	1.651	1.270
Bend degree	90	90
Radius of curvature, $R_c$ (mm)	4.053	3.823
Radius ratio, $2R_c/D_h$	6.8	9.1
Tube length, L (mm)	100	100

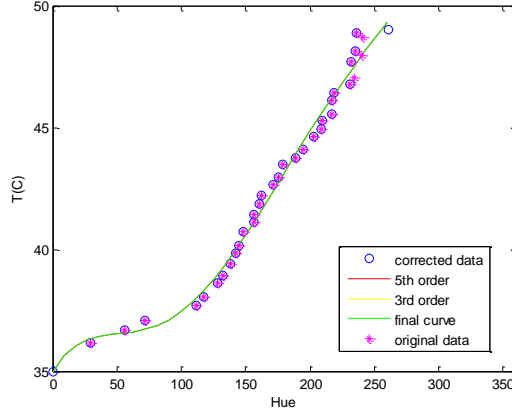


Fig. 2. Calibration curve fitting done by MATLAB ( $D_h = 1.194$  mm,  $Re = 5000$ ,  $q'' = 6$  kW/m<sup>2</sup>)

### 2. 3. Data Reduction and Uncertainties

The local heat transfer coefficient  $h_x$  and the local Nu number  $Nu_x$  are calculated by,

$$h_x = \frac{q''}{T_{w,in,x} - T_{f,x}} \quad (1)$$

Where  $T_{w,in,x}$  is the local inner wall temperature, and  $T_{f,x}$  is the local bulk flow temperature.

$$T_{w,in,x} = T_{w,out,x} + \frac{\dot{e}(D_{out}^2 - D_h^2)}{16K_{tube}} + \left( \frac{\dot{e}D_{out}^2}{8K_{tube}} - \frac{q''_{loss}D_{out}}{2K_{tube}} \right) \ln\left(\frac{D_h}{D_{out}}\right) \quad (2)$$

$$\dot{e} = \frac{4VI}{\pi(D_{out}^2 - D_h^2)L_h} \quad (3)$$

$T_{f,x}$  can be calculated based on energy balance equation,

$$\dot{Q} \frac{x}{L_h} = \dot{m} C_p (T_{f,x} - T_{in}) \quad (4)$$

$$Nu_x = \frac{h_x x}{K_f} \quad (5)$$

Where  $Q$  is the DC power less the heat loss,  $\dot{Q} = V \times I - \dot{Q}_{loss}$ ,  $x$  is the local position interested along the test microtube center line.  $C_p$  is the specific heat of FC-72, which is a function of temperature (3M Company). Once  $T_{f,x}$  is calculated, the local Nu number ( $Nu_x$ ) can be obtained from its definition (Eq.5). The heat loss estimation method is similar to Fan and Hassan (2013). In current study, the maximum heat loss is 12%, and decreases as the heat flux increases.

The uncertainty of TLC measurement is determined by the method from Muwaga and Hassan (2006). Besides, the uncertainty due to the tube bending deformation needs to be discussed. Mentella and Strano (2012) did numerical and experimental studies on free rotary draw bending for small diameter tubes with thin walls. They noted that this bending technique caused the cross-section deformation and the flow area shrinks; therefore, the cross-section ovalization at curved portion might cause extra pressure drop other than due to the secondary flow itself. In the current study, the tested microtube is bended by the same

technique, and the cross-section area is inevitably and unavoidably changed (Fig. 3). Mentella and Strano (2012) also mentioned the most obvious deformation occurred at the half way of bending angle, and introduced the ovalization O% (Eq.6) to describe the cross section deformation level. In current study, both curved microtubes have large deformation which affects the heat transfer measurement since the calculations are based on ideal shape channels. Thus, the uncertainty of Nu number is quite large. The uncertainties in this experiment are listed in Table. 2.

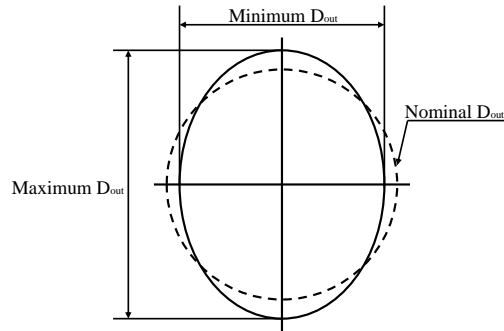


Fig. 3. Bended tube ovalization schematic

$$\text{Ovalization (O\%)} = \frac{(\text{Maximum } D_{\text{out}} - \text{Minimum } D_{\text{out}})}{\text{Nominal } D_{\text{out}}} \times 100\% \quad (6)$$

Table. 2. Uncertainties

Measurement Parameters	Uncertainty
TLC temperature, $T_w$	1.1 °C
T-type thermocouples, T	± 0.5 °C
Volumetric flow rate, Q,	± 8.72 ml/min
Voltage, V	± 0.05 V
Current, I	± 0.05 A
Outer diameter of microtube, $D_{\text{out}}$	± 0.0127 mm
Ovalization, %	11.8% (Tube #1), 15.8% (Tube #2)
Calculated Parameters	Uncertainty
Temperature difference, $\Delta T$	1.21 °C
Heat flux, $q''$	± 0.9 ~ 1.5 kW/m <sup>2</sup>
Local Nusselt number, Nu	29%

### 3. Results and Discussion

#### 3. 1. Surface Temperature Map

In Fig. 4 (a), an example of HUE image captured by the CCD camera for the heat transfer investigation is exhibited. Fig. 4 (b) is the corresponding surface temperature map obtained by MATLAB, and the arrow points the flow direction. It shows when the working flow enters the curved portion, the surface temperature drop, which implies the increased heat transfer coefficient. The details will be discussed below. Moreover, the surface temperature map exhibits the curved shape contribution on the

heat transfer enhancement; therefore, TLC is applicable for temperature measurement in compact areas with complicated shapes.

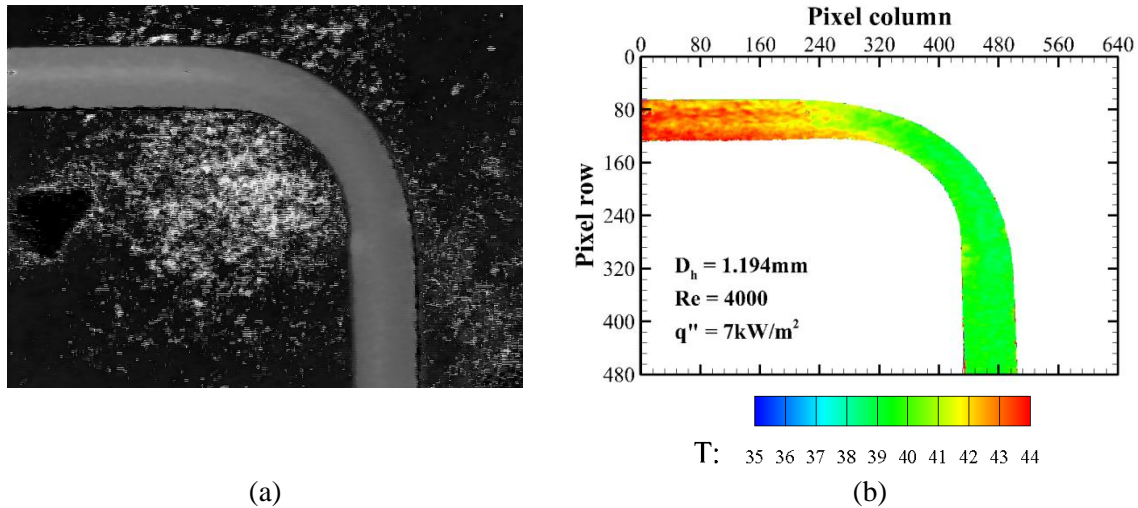


Fig. 4. (a) An example of HUE image and (b) the corresponding surface temperature map

### 3. 2. Single-Phase Liquid Heat Transfer

Fig. 5 (a) and (b) presents the stream-wise local Nu number against  $x/D_h$  at two Re number 4000 and 5500, which is the stream-wise dimensionless distance with respect to the hydraulic diameter  $D_h = 1.194$  mm in ROI. Set  $x_0/D_h = 0$  at the heated length beginning (Fig. 1 (b)). Between  $x/D_h = 22.5$  and 27, the working liquid is in the upstream straight portion, and enters the curved portion ( $x/D_h = 27$  to 32), and then flows to downstream straight portion. At all Re, the local Nu number is enhanced in the curved portion. As the flow entering the straight downstream, the enhancement is reduced. When the flow entering the curved portion, because of the centrifugal force, the fluid particles in the channel center region move towards to the concave wall so that the pressure there is higher than the convex side; namely, a radial pressure gradient is formed. The flow speed is reduced when closed to the wall because of the no-slip condition. The radial pressure gradient, then, drives the fluid turns back to the convex side along the wall surface. Eventually, the secondary flow vortices generated in the plane which is perpendicular to the curved tube axis. This flow feature helps the heat transfer enhancement, however, as the flow left the curved portion, the secondary flow effect reduced (Dean Vortices become weaker and weaker), and may finally disappear when travelled further to the downstream straight portion. Dravid et al. (1971) conducted experiments in helically coil tubes to study the heat transfer behaviour in laminar flow due to the secondary flow effect. They had the similar observation that the wall temperature showed spatial oscillations during the developing flow and vanish in the fully developed region. In current study, the 90 degree bend microtube can be considered as a quarter of coiled tube at the very beginning where the flow is developing. Therefore, in current case, the local Nu number  $Nu_x$  also shows spatial oscillation trends as Dravid mentioned due to the wall temperature oscillation caused by the secondary flow effect. Three existing Nu number correlations (Dravid et al., 1971; Rogers and Mayhew, 1964; Manlapaz and Churchill, 1980) are plotted in Fig. 5. Although all three correlations were considered Dean Vortices effect, they were generated based on the fully developed flow in helically coiled to predict the average Nu value. In current experiments, via TLC technique, the continuous local Nu number can be obtained as Fig. 5 shown. Moreover, the local Nu number in curved portion depends not only on De number (how strong the secondary flow is), but also on the turning angle  $\theta$  (the location of the flow), and the detail will be discussed later. In addition, in Fig. 5 (b), when  $q'' = 5$  kW/m<sup>2</sup> applied, the results leave apart from the group. It may be because when the flow rate is fast and the applied heat flux is small, the heat transfer

coefficient is usually high, and the tube surface is relatively cooled well. Therefore, this is a challenge to use TLC for measuring at this kind of critical operating conditions.

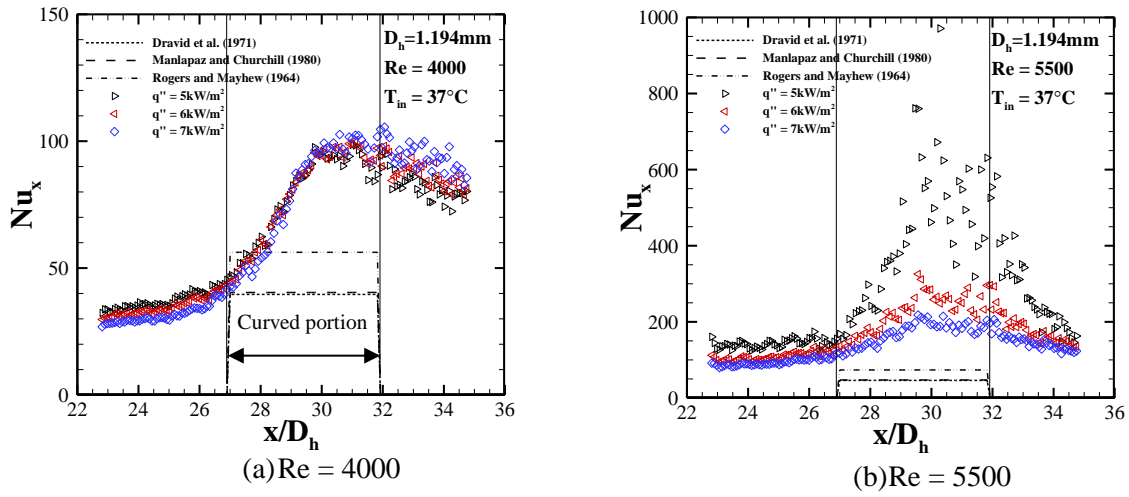


Fig. 5. Local Nusselt number from experiments along the flow direction applied by different  $q''$  at (a)  $Re=4000$  and (b)  $Re=5500$  and compared with the well-known correlations in curved shape.

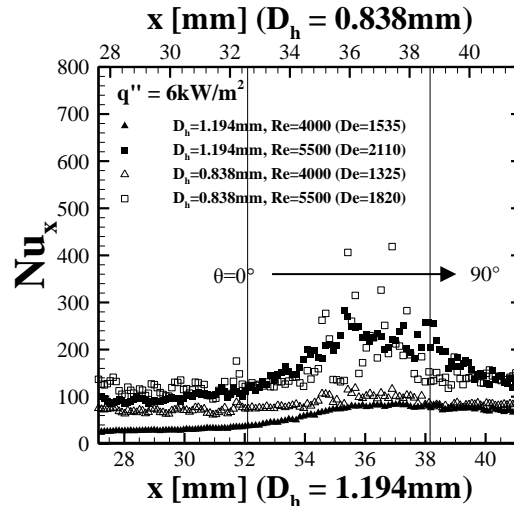


Fig. 6. Local heat transfer comparison between two microtubes at the same heat flux  $q'' = 6\text{ kW/m}^2$

Fig. 6 shows the comparison of the local Nu number  $Nu_x$  for both sizes of microtubes along the flow direction by coinciding the curved portions (the region between two parallel lines refers the turning angle  $\theta$  varies from  $0^\circ$  to  $90^\circ$ ) at different heat fluxes. The maximum local Nu number is observed between  $\theta = 40^\circ$  and  $60^\circ$  from the inlet of curved portion depending on the hydraulic diameter and the De number. Taylor et al. (1982) conducted experiments in a  $90^\circ$  bend duct (radius ratio = 2.3) with water to investigate the secondary motion behaviour under developing laminar and turbulent flow. They concluded that the bend affects the velocity profile with respect to the turning angle. The location of the maximum velocity moves gradually from the center of the duct to the wall as the fluid goes further in the bend. The authors observed that around  $\theta = 60^\circ$ , the strongest Dean vortices worked with the axial velocities to remove the hot fluid away from the wall and guide the cooler one from the center region. Thus, the heat transfer enhancement was maximized. In current case, when the heat flux is applied at  $6\text{ kW/m}^2$ , as De

number increases, the maximum Nu number occurs earlier in each size of microtube due to the enhanced Dean Vortices. However, as the hydraulic diameter reduces, the increased De number has less effect on the heat transfer enhancement, and the reason may be due to large pressure drop in the curved portion. Compared to the peak, the heat transfer enhancement near the inlet region doesn't show obviously. Dravid et al. (1971) introduced a ratio called  $\theta$ -average Enhancement factor E (Eq.7) to discuss the local heat transfer at the inlet of the coiled tube compared to that in a straight tube.

$$\dot{E} = 0.447De^{1/6} \quad (7)$$

Based on Eq.4, in current study, as  $De = 1325$ ,  $\dot{E} = 1.48$ , as  $De = 2110$ ,  $\dot{E} = 1.6$ . The authors had a similar finding and concluded that at the beginning of curved portion, the heat transfer enhancement due to the secondary flow was not significantly because of the thermal boundary layer was very thin there and not strong enough to deliver the heat from wall surface to go through the secondary flow field and then leave with the main flow. As the fluid passing the bend continuously, the thermal boundary layer grew which meant the secondary flow worked better to enhance the heat transfer coefficient, and the enhancement factor increased gradually up to  $De^{1/2}$  times dependence in the fully developed region. The trends in Fig. 6 are coincident with the previous discussion, but because of the developing laminar flow in the current study, the enhancement factor is not large compared to the case in fully developed flow. Then, as the flow closes to the exit of the bend, the secondary flow effect on heat transfer is reduced, and may finally vanish.

#### 4. Conclusion

In this paper, the single-phase liquid heat transfer in single 90° curved microtube with small curvature radius has been investigated using TLC measurement. The experimental results show that the heat transfer coefficient in curved microtube is enhanced because of the secondary flow effect. Moreover, the enhancement relates to the turning angle, and the maximum Nu number occurs earlier as the De number increases in the range of the turning angle of 40° to 60°. The heat transfer enhancement in large hydraulic diameter is better. The TLC methodology showed good performance to measure surface temperature on compact curved shape. However, some difficulties need to be overcome, such as coating quality and bad pixels filtering. The uncertainty due to the test section deformation has to be reduced in future studies.

#### References

- Al-Halhouli A., Biittgenbach S. (2010). Liquid Flow in Curved Microchannels. *International Journal of Theoretical and Applied Multiscale Mechanics*, 1, 253-265.
- Chu J., Teng J., Xu T., Huang S., Jin S., Yu X., Dang T., Zhang C., Greif R. (2012). Characterization of Frictional Pressure Drop of Liquid Flow through Curved Rectangular Microchannels. *Experimental Thermal and Fluid Science*, 38, 171-183.
- Dean W. R. (1927). Note on the Motion of Fluid in a Curved Pipe. London, Edinburgh, and Dublin, *Philosophical Magazine and Journal of Science*, 4, 208-223.
- Dean W. R. (1928). The Stream-Line Motion of Fluid in a Curved Pipe. London, Edinburgh, and Dublin, *Philosophical Magazine and Journal of Science*, 5, 673-695.
- Dravid A. N., Smith K. A., Merrill E. W., Brian P. L. T. (1971). Effect of Secondary Fluid Motion on Laminar Flow Heat Transfer in Helically Coiled Tubes. *AIChE Journal*, 17, 1114-1122.
- Fan Y., Hassan I. (2013). Effect of Inlet Restriction on Flow Boiling Heat Transfer in a Horizontal Microtube. *Journal of Heat Transfer*, 135, 021502 (9pp.).
- Manlapaz R. L., Churchill S. W. (1980). Fully Developed Laminar Flow in A helically Coiled Tube of Finite Pitch. *Chemical Engineering Communications*, 7, 57-78.
- Mentella A., Strano M. (2012). Rotary Drawing Bending of Small Diameter Copper Tubes: Predicting the Quality of the Cross-Section. *Proc. Inst. Mech. Eng. Pt. B: J. Eng. Manuf.*, 226, 267-278.

- Mori Y., Nakayama W. (1965). Study on Forced Convective Heat Transfer in Curved Pipes. *International Journal of Heat and Mass Transfer*, 8, 67-82.
- Mori Y., Uchida Y., Ukon T. (1971). Forced Convective Heat Transfer in a Curved Channel with a Square Cross Section. *International Journal of Heat and Mass Transfer*, 14, 1787-1805.
- Mudawar I. (2011). Two-phase Microchannel Heat Sinks: Theory, Applications, and Limitations. 133, 041002 (33pp.).
- Muwanga R., Hassan I. (2006). Local Heat Transfer Measurements in Microchannels using Liquid Crystal Thermography: Methodology Development and Validation. *Journal of Heat Transfer*, 128, 617-626
- Rogers G. F. C., Mayhew Y. R. (1964). Heat Transfer and Pressure Loss in Helically Coiled Tubes with Turbulent Flow. *International Journal of Heat and Mass Transfer*, 7, 1027-1216.
- Sturgis J. C., Mudawar I. (1999). Single-Phase Heat Transfer Enhancement in a Curved, Rectangular Channel Subjected to Concave Heating. *International Journal of Heat and Mass Transfer*, 42, 1255-1272.
- Taylor A. M. K. P., Whitelaw J. H., Yianneskis M. (1982). Curved Ducts with Strong Secondary Motion: Velocity Measurements of Developing Laminar and Turbulent Flow. *Journal of Fluids Engineering*, 104, 350-359.
- Xi Y., Yu J., Xie Y., Gao H. (2010). Single-Phase Flow and Heat Transfer in Swirl Microchannels. *Experimental Thermal and Fluid Science*, 34, 1309-1315.
- Yang W., Zhang J., Cheng H. (2005). The Study of Flow Characteristics of Curved Microchannel. *Applied Thermal Engineering*, 25, 1894-1907.